Structural Engineering and Mechanics, *Vol. 57, No. 1 (2016) 179-200*
DOI: http://dx.doi.org/10.12989/sem.2016.57.1.179

An investigation into the influence of thermal loading and surface effects on mechanical characteristics of nanotubes

Farzad Ebrahimi*, Gholam Reza Shaghaghi and Mahya Boreiry

Mechanical Engineering Department, Faculty of Engineering, Imam Khomeini International University, Qazvin, P.O.B. 16818-34149, Iran

(Received November 14, 2014, Revised December 15, 2015, Accepted December 16, 2015)

Abstract. In this paper the differential transformation method (DTM) is utilized for vibration and buckling analysis of nanotubes in thermal environment while considering the coupled surface and nonlocal effects. The Eringen's nonlocal elasticity theory takes into account the effect of small size while the Gurtin-Murdoch model is used to incorporate the surface effects (SE). The derived governing differential equations are solved by DTM which demonstrated to have high precision and computational efficiency in the vibration analysis of nanobeams. The detailed mathematical derivations are presented and numerical investigations are performed while the emphasis is placed on investigating the effect of thermal loading, small scale and surface effects, mode number, thickness ratio and boundary conditions on the normalized natural frequencies and critical buckling loads of the nanobeams in detail. The results show that the surface effects lead to an increase in natural frequency and critical buckling load of nanotubes. It is explicitly shown that the vibration and buckling of a nanotube is significantly influenced by these effects and the influence of thermal loadings and nonlocal effects are minimal.

Keywords: nanotube, surface effects; nonlocal elasticity theory; thermal effect; critical buckling load; differential transformation method

1. Introduction

In recent years, nanomechanical and nano-electro-mechanical systems (NEMS) at nanoscale receive special attention from researchers. Among them nanobeams attracted more attention because of their potential usage (Eltaher *et al*. 2013). For difficulty of experiments at nanoscale, the mechanical behaviors of the nanostructures are usually investigated using mathematical simulations such as atomistic, atomistic-continuum mechanics and continuum mechanics approaches. Since performing atomistic and atomistic-continuum mechanics simulations in large scales experiments need much time and expenses, continuum mechanic approaches are often used (Malekzadeh *et al*. 2013).

In the classical continuum theory the small scale effect and size dependence of material properties cannot be predicted, but in continuum approaches nonlocal effect can be simulated (Hosseini-Hashemi *et al*. 2013a). The nonlocal effect which first considered by Eringen expresses

*Corresponding author, Professor, E-mail: febrahimy@eng.ikiu.ac.ir

http://www.techno-press.org/?journal=sem&subpage=8 ISSN: 1225-4568 (Print), 1598-6217 (Online)

that in continuum the stress in one point is the function of strains in all points in the bulk of material (Wang *et al*. 2006, Ansari *et al*. 2012). Reddy (2007) computed motion equations with considering nonlocal effect for different beam theories and described nonlocal effect on natural frequencies, buckling loads, deflections. Wang *et al*. (2007a) studied the nonlocal effect on vibration of nanobeams based on TBT. From their observations this effect has dominant role in stubby beam and also in high frequencies. Thai *et al*. (2012) obtained motion equations by considering the nonlocal effect on bending, buckling and vibration of nanobeams based on Euler-Bernoulli beam theory for just simply boundary condition. They indicated that as this effect increases, the rate of drop of frequency with nonlocal parameter is magnified for higher modes.

In studying nanoscale structures, the molecular effects which exist in this scale are undeniable, such as the surface effects. The surface of a solid has different property from the bulk which is considerable in nanoscale and this effect has dominant influence on frequency in nanoscale (Malekzadeh *et al*. 2013). The Young's modulus of macroscopic materials is not size-dependent, but in nanoscale this modulus is size-dependent. The surface effects which affected from the elastic modulus depend on the size of the structures, too. In macroscale they can be neglected while in nanoscale because of the large surface to volume ratio they have significant role (Guo *et al*. 2007). Many studies considered surface effects in the dynamic analysis of nanostructures such as Gheshlaghi *et al*. (2011), Wang *et al*. (2007) and also Hosseini-Hashemi *et al*. (2013b).

In few studies the surface and nonlocal effects investigated simultaneously. Most recently, Eltaher *et al*. (2013) studied the coupling effects of nonlocal and surface energy on free vibration of nanobeam based on EBT. They concluded that the surface effects depend on the size and the material of the nanobeam by calculating natural frequencies for two different materials. Hosseini *et al*. (2013a) studied the surface and nonlocal effects on free vibration of nanobeam based on both EBT and TBT by using analytical method for various boundary conditions. They showed that the rotary inertia and shear deformation reduce the surface effects on the natural frequencies. In a similar study, Ebrahimi *et al*. (2015a) studied surface and nonlocal effects on buckling and vibrational characteristics of nanotubes with differential transformation method.

In addition, investigating the thermal effect in dynamic analysis of nanotubes is necessary. The thermal effect provides an axial load which result to bending and buckling in nanotubes. Few studies considered thermal effect in vibration and buckling analysis of nanotubes such as Zhang *et al*. (2007), Wang *et al*. (2008) and Amirian *et al*. (2014). And also Ebrahimi *et al*. (2015b) studied the effect of various thermal loadings on buckling and vibrational characteristics of nonlocal FG nanobeams. They indicated that the proposed modeling can provide accurate frequency results of the FG nanobeams. Moreover, Shariyat (2009) investigated the dynamic buckling of piezo-laminated plates under thermo-electro-mechanical loads with consideration of the temperature dependency of the material properties.

The governing motion equations are often solved by analytical method such as Reddy (2007) and Hosseini-Hashemi *et al*. (2013a) or finite element methods such as Eltaher *et al*. (2013) or generalized differential quadrature (GDQ) method like Malekzadeh *et al*. (2013) and other solutions which need high CPU time to solve. DTM method a semi-analytical-numerical technique which comes from Taylor's series expansion is simpler and has better precision in compare with other methods. This method was first expresses by Zhou (1987) for electrical circuits. In contrast with the Taylor series method which is needed long computation time in large orders, in this method the accurate results with good precision can be obtained. The exact solution of both linear and nonlinear equations and even partial differential equations can be solved by this method such as Abazari *et al*. (2012). In other words, by applying DTM, governing equations for various

boundary conditions reduces to algebraic equations, and finally all the calculations turn into simple iterative process (Abbasi *et al*.2014).

Moreover, although the dynamic analysis of nanotubes by considering surface and nonlocal effects is studied, but the thermal effects on the natural frequencies and buckling loads is not considered in these studies. To the best knowledge of the authors, no research has been found to study the buckling and vibration analysis of nanotubes characteristics by considering surface and small scale effects in presence of thermal effect for various boundary conditions by employing DTM. The approximate expressions of natural frequencies and buckling loads based on Hamilton's method in the framework of Euler-Bernoulli beam theory for Aluminum and Silicon nanotubes are obtained. Comparisons with the results from the well-known references with good agreement between the results of the DTM method and those available in literature validated the presented approach. It is demonstrated that the DTM has high accuracy and precision in dynamic analysis of nanotubes.

2. Theory and formulation

2.1 Nonlocal elasticity theory

According to Eringen (1983) in an elastic continuum the stress field at one point depends on strains of all points in the bulk. This effect can be justified by the atomic theory of lattice dynamics and phonon dispersions' researches. The nonlocal tensor σ_{ij} can be expressed as (Reddy 2007)

$$\sigma_{ij}(x) = \int_{\Omega} \alpha(|x' - x|, \tau)\, t_{ij}(x')\, d\Omega(x') \tag{1}$$

where t_{ij} (x') are the components of the classical local stress tensor at point x which are related to the components of the linear strain tensor ε_{kl} by the conventional constitutive relations for a Hookean material, i.e.

$$t_{ij} = C_{ijkl}\varepsilon_{kl} \tag{2}$$

The meaning of Eq. (1) is that the nonlocal stress at point x is the weighted average of the local stress of all points in the neighborhood of x, the size of which is related to the nonlocal kernel $\alpha(|x'-x|, \tau)$. Here $|x'-x|$ is the Euclidean distance and τ is a constant which depends on the bulk's material and both internal and external characteristic lengths like lattice spacing and wavelength which can be obtained as

$$\tau = \frac{e_0 a}{l} \tag{3}$$

Which represents the ratio between a characteristic internal length, a (such as lattice parameter, C-C bond length and granular distance) and a characteristic external one, l (e.g., crack length, wavelength) through an adjusting constant e_0, dependent on each material. The magnitude of e_0 is determined experimentally or approximated by matching the dispersion curves of plane waves with those of atomic lattice dynamics.

For difficulty of integral form of Eq. (1) in motion equations, the differential form is represented as follows (Eringen *et al*. 1972)

$$(1-(e_0a)\nabla^2)\sigma_{kl}=t_{kl} \tag{4}$$

Here ∇^2 is the Laplacian operator. Moreover, the scale length e_0a takes into account the size effect on the response of nanostructures. In a one-dimensional case, for an elastic material the constitutive relations will be simplified as follows (Miller *et al*. 2000)

$$\sigma_{xx}-\mu\frac{\partial^2\sigma_{xx}}{\partial x^2}=E\,\varepsilon_{xx} \tag{5}$$

where σ and ε are the nonlocal stress and strain respectively, $\mu=(e_0a)^2$ is nonlocal parameter, E is the elasticity modulus.

2.2 Surface effect theory

The energy which associated by atoms in surface layers is different from the atoms in the bulk of material, which is called surface free energy. In most study this energy is neglected because it is introduced with a few layers of atoms near the surface, but in nanosize this energy cannot be ignored (He *et al*. 2004). In nanoscale this effect has dominant influence because of its high ratio of surface to volume which the result is the higher elastic modulus and mechanical strength than classical studies. The curvature of a bending beam can be approximated by $\partial^2w/\partial x^2$. The Laplace-Young equation (Wang and Feng 2009) in Eq. (6) indicates that for a bending beam $\partial^2w/\partial x^2$, the distributed transverse loading induced by the residual surface stress is

$$q=q_0+H\frac{\partial^2w}{\partial x^2} \tag{6}$$

Here the parameter H is a constant determined by the residual surface stress and the shape of cross section. For circular cross sections, H is given, respectively, by

$$H=2\tau^oD \tag{7}$$

where τ^o is the residual surface stress under unstrained condition, and effective flexural rigidity, EI^*, for nanotube is given by

$$EI^*=\frac{1}{4}\pi E(R_o^4-R_i^4)+\pi E^s(R_o^3+R_i^3) \tag{8}$$

where E^s is the surface elastic modulus which can be determined by atomistic simulations or experiments and inner and outer radii R_i and R_o is considered, respectively.

2.3 Euler-Bernoulli beam theory

The motion equation is obtained by EBT which is based on the displacement of beam components. In this theory the straight vertical lines in the mid-plane remain straight after deformation. And the shear deformation and rotational inertia are not assumed .The strain-displacement equations for EBT can be described as follows

$$u_1=u(x,t)-z\frac{\partial w}{\partial x}\quad,\quad u_2=0\quad,\quad u_3=w(x,t) \tag{9}$$

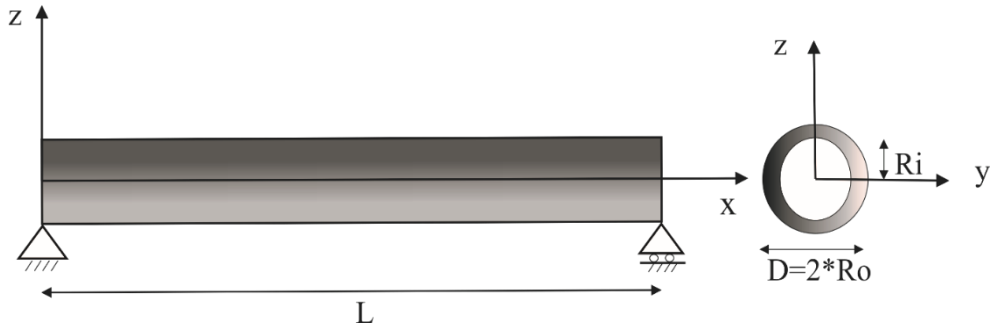

Fig. 1 Geometry of a nanotube with Length L, inner and outer radii R_i and R_o

In the above equation (u,w) are axial and transverse displacements of a point on mid-plane of the beam, respectively. And the nonzero strains can be described as

$$\varepsilon_{xx} = \frac{\partial u}{\partial x} - z\frac{\partial^2 w}{\partial x^2} \quad , \quad \gamma_{xz} = \frac{\partial u_1}{\partial x} + \frac{\partial u_2}{\partial x} = 0 \tag{10}$$

The governing equations of motion and the boundary conditions for EBT can be derived by Hamilton's principles as follows

$$\int_0^t \delta(T - U + V)dt = 0 \tag{11}$$

Here U is the strain energy, T is the kinetic energy and V is work done by external forces.
The first variation of the strain energy can be calculated as

$$\delta U = \int_v \sigma_{ij}\delta\varepsilon_{ij}dV = \int_v (\sigma_{xx}\delta\varepsilon_{xx})dV \tag{12}$$

Substituting Eq. (10) into Eq. (12) yields

$$\delta U = \int_0^L \left[N\delta\left(\frac{\partial u}{\partial x}\right) - M\delta\left(\frac{\partial^2 w}{\partial x^2}\right)\right]dx \tag{13}$$

where N and M are the axial force and bending moment respectively. These stress resultants used in Eq. (13) are defined as

$$N = \int_A \sigma_{xx}dA, \quad M = \int_A \sigma_{xx}z\,dA \tag{14}$$

The kinetic energy for EBT can be written as

$$T = \frac{1}{2}\int_0^L \int_A \rho\left(\left(\frac{\partial u_1}{\partial t}\right)^2 + \left(\frac{\partial u_3}{\partial t}\right)^2\right)dA\,dx \tag{15}$$

And the first variation of the Eq.(15) can be obtained as

$$\delta T = \int_0^L \left[\rho A\frac{\partial u}{\partial t}\delta\left(\frac{\partial u}{\partial t}\right) + \rho A\frac{\partial w}{\partial t}\delta\left(\frac{\partial w}{\partial t}\right) + \rho I\frac{\partial^2 w}{\partial t\,\partial x}\delta\left(\frac{\partial^2 w}{\partial t\,\partial x}\right)\right]dx \tag{16}$$

where ρ, I, A are the mass density, moment inertia and cross sectional area of the nanotube respectively. The first variation of external forces work of the beam can be written in the form

$$\delta V = \int_0^L \left(f\,\delta u + q\delta w \right) dx \tag{17}$$

In which f and q are external axial and transverse loads distribution along length of beam, respectively. Substituting Eqs. (13), (16) and (17) into Eq. (11) and setting the coefficients of $\delta u, \delta w$ and $\delta(\frac{\partial w}{\partial x})$ to zero, lead to the following motion equations

$$\frac{\partial N}{\partial x} + f = \rho A \frac{\partial^2 u}{\partial t^2} \tag{18a}$$

$$\frac{\partial^2 M}{\partial x^2} - \frac{\partial}{\partial x}\left(\bar{N} \frac{\partial w}{\partial x} \right) + q = \rho A \frac{\partial^2 w}{\partial t^2} - \rho I \frac{\partial^4 w}{\partial t^2 \partial x^2} \tag{18b}$$

Integrating Eq. (5) over the beam's cross-section area, we obtain the force-strain and the moment-strain of the nonlocal EBT can be obtained as follows

$$N - \mu \frac{\partial^2 N}{\partial x^2} = EA \frac{\partial u}{\partial x} \tag{19a}$$

$$M - \mu \frac{\partial^2 M}{\partial x^2} = -EI^* \frac{\partial^2 w}{\partial x^2} \tag{19b}$$

The explicit relation of the nonlocal normal force and bending moment can be derived by substituting for the second derivative of M from Eq. (18) into Eq. (19) as follows

$$N = EA \frac{\partial u}{\partial x} + \mu \left(\frac{\partial^3 u}{\partial x \partial t^2} - \frac{\partial f}{\partial x} \right) \tag{20a}$$

$$M = -EI^* \frac{\partial^2 w}{\partial x^2} + \mu \left(\frac{\partial}{\partial x}\left(\bar{N} \frac{\partial w}{\partial x} \right) - q + \rho A \frac{\partial^2 w}{\partial t^2} - \rho I \frac{\partial^4 w}{\partial t^2 \partial x^2} \right) \tag{20b}$$

The nonlocal governing equations of Euler-Bernoulli nanotubes in terms of the displacement can be derived by substituting for N and M from Eq. (20) into Eq. (18) as follows

$$\frac{\partial}{\partial x}\left(EA \frac{\partial u}{\partial x} \right) + f - \mu \frac{\partial^2 f}{\partial x^2} = \rho A \frac{\partial^2 u}{\partial t^2} - \mu \rho A \frac{\partial^4 u}{\partial t^2 \partial x^2} \tag{21a}$$

$$\begin{aligned} &\frac{\partial^2}{\partial x^2}\left(-EI^* \frac{\partial^2 w}{\partial x^2} \right) + \mu \frac{\partial^2}{\partial x^2}\left[\frac{\partial}{\partial x}\left(\bar{N} \frac{\partial w}{\partial x} \right) - q_0 - H \frac{\partial^2 w}{\partial x^2} + \rho A \frac{\partial^2 w}{\partial t^2} - \rho I \frac{\partial^4 w}{\partial t^2 \partial x^2} \right] + q_0 + H \frac{\partial^2 w}{\partial x^2} \\ &- \frac{\partial}{\partial x}\left(\bar{N} \frac{\partial w}{\partial x} \right) = \rho A \frac{\partial^2 w}{\partial t^2} - \rho I \frac{\partial^4 w}{\partial t^2 \partial x^2} \end{aligned} \tag{21b}$$

When the nanotube vibrates with a natural frequency ω, it is possible to separate the time dependency by expressing the displacement parameters in the following form

$$w(x,t) = W(x)e^{i\omega t} \tag{22}$$

Substituting harmonic vibration modes of Eq. (22), into Eq. (21) leads to a time-independent governing equation as follows

$$\begin{aligned} &\frac{\partial^2}{\partial x^2}\left(-EI^* \frac{\partial^2 W}{\partial x^2}\right) + \mu \frac{\partial^2}{\partial x^2}\left[\frac{\partial}{\partial x}\left(\bar{N}\frac{\partial W}{\partial x}\right) - q_0 - H\frac{\partial^2 w}{\partial x^2} - \rho A\omega^2 W + \rho I\omega^2 \frac{\partial^2 W}{\partial x^2}\right] + q_0 + H\frac{\partial^2 w}{\partial x^2} \\ &-\frac{\partial}{\partial x}\left(\bar{N}\frac{\partial W}{\partial x}\right) = \rho I\omega^2 \frac{\partial^2 W}{\partial x^2} - \rho A\omega^2 W \end{aligned} \tag{23}$$

where E is Young's modulus, I second moment of area about the y-axis, w the deflection of the beam, ρ density of the nanobeam, A cross section area of the nanobeam, L nanobeam length and $\bar{N}$ represents the axial force on the nanobeam and is expressed as

$$\bar{N} = N_m + N_\theta \tag{24}$$

where N_m and N_θ are the axial force due to the mechanical loading prior to buckling and axial force due to the influence of temperature change, respectively. The thermal axial force N_θ can be written as (Zhang *et al*. 2008)

$$N_\theta = -\frac{E\,A}{1-2\nu}\alpha_x \theta \tag{25}$$

where α_x is the coefficient of thermal expansion in the direction of X-axis, v is Poisson's ratio and θ denotes the change in temperature.

3. Differential transformation method

Several methods are used for solving resultant motion equations as finite element method, Galerkin method or analytical methods. These methods are so common but they need high CPU time to solve. DTM is one of the solving methods which has some advantages in compare with others as converging the value with acceptable precision and can be used for linear and non-linear equations for various boundary conditions. The basic definitions can be expressed as follows. In this method, differential transformation of k the derivative function $y(x)$. This method transform the differential equations and boundary conditions into algebraic equations and also a closed-form series solution can be obtained. In Tables 1 and 2 some transformation rules are presented to both the differential equations and the boundary conditions. The basic definitions and the application procedure of this method can be introduced as follows. The transformation equation of function can be defined as (Chen and Ju 2004)

$$F[k] = \frac{1}{k!}\left(\frac{d^k f(x)}{dx^k}\right)_{x=x_0} \tag{26}$$

where $f(x)$ the original is function and $F[k]$ is the transformed function. The inverse transformation

Table 1 Some of the transformation rules of the one-dimensional DTM

Original function	Transformed function
$f(x)=g(x)\pm h(x)$	$F(K)=G(K)\pm H(K)$
$f(x)=\lambda g(x)$	$F(K)=\lambda G(K)$
$f(x)=g(x)\,h(x)$	$F(K)=\sum_{l=0}^{K} G(K-l)H(l)$
$f(x)=\frac{d^n g(x)}{dx^n}$	$F(K)=\frac{(k+n)!}{k!}G(K+n)$
$f(x)=x^n$	$F(K)=\delta(K-n)=\begin{cases}1 & k=n\\ 0 & k\neq n\end{cases}$

Table 2 Transformed boundary conditions (B.C.) based on DTM

$X=0$		$X=L$	
Original B.C.	Transformed B.C.	Original B.C.	Transformed B.C.
$f(0)=0$	$F(0)=0$	$f(L)=0$	$\sum_{k=0}^{\infty} F[k]=0$
$\frac{df(0)}{dx}=0$	$F(1)=0$	$\frac{df(L)}{dx}=0$	$\sum_{k=0}^{\infty} k\,F[k]=0$
$\frac{d^2 f(0)}{dx^2}=0$	$F(2)=0$	$\frac{d^2 f(L)}{dx^2}=0$	$\sum_{k=0}^{\infty} k(k-1)F[k]=0$
$\frac{d^3 f(0)}{dx^3}=0$	$F(3)=0$	$\frac{d^3 f(L)}{dx^3}=0$	$\sum_{k=0}^{\infty} k(k-1)(k-2)F[k]=0$

is defined as

$$f(x)=\sum_{k=0}^{\infty}(x-x_0)^k F[k] \tag{27}$$

Combining Eqs. (26) and (27) one obtains

$$f(x)=\sum_{k=0}^{\infty}\frac{(x-x_0)^k}{k!}\left(\frac{d^k f(x)}{dx^k}\right)_{x=x_0} \tag{28a}$$

In actual application, the function $f(x)$ is expressed by a finite series and Eq. (28a) can be written as follows

$$f(x)=\sum_{k=0}^{N}\frac{(x-x_0)^k}{k!}\left(\frac{d^k f(x)}{dx^k}\right)_{x=x_0} \tag{28b}$$

Which implies that the term in relation (28c) is negligible

$$f(x)=\sum_{k=N+1}^{\infty}\frac{(x-x_0)^k}{k!}\left(\frac{d^k f(x)}{dx^k}\right)_{x=x_0} \tag{28c}$$

4. Implementation of differential transformation method

The Eq. (23) is solved by DTM approach and solving the complicated transcendental algebraic equations for general boundary conditions will be simplified. By applying differential transformation method to Eq. (23) and using Table 1 the resultant equation has the following form:

• Vibration equation

$$\begin{aligned}&(EI^{*}+\mu H-\mu\rho I\omega^{2}-\mu\bar{N})\frac{(k+4)!}{k!}\ W[k+4]\\&+\left(\mu\rho A\omega^{2}+\rho I\omega^{2}-H+\bar{N}\right)\frac{(k+2)!}{k!}\ W[k+2]-\rho A\omega^{2}\ W[k]=0\end{aligned} \tag{29a}$$

• Critical buckling load equation

$$(EI^{*}+\mu H-\mu\bar{N})\frac{(k+4)!}{k!}\ W[k+4]+\left(\bar{N}-H\right)\frac{(k+2)!}{k!}\ W[k+2]=0 \tag{29b}$$

where $W[k]$ is the transformed functions of w. Also the various boundary condition for nanotubes by using Table 2 can be expressed as follows:

Simply supported-Simply supported:

$$\begin{aligned}&W[0]=0,\ W[2]=0\\&\sum_{k=\rho}^{\infty}W[k]=0,\ \sum_{k=0}^{\infty}k[k-1]W[k]=0\end{aligned} \tag{30a}$$

Clamped-Clamped:

$$\begin{aligned}&W[0]=0,\ W[1]=0\\&\sum_{k=0}^{\infty}W[k]=0,\ \sum_{k=0}^{\infty}k\ W[k]=0\end{aligned} \tag{30b}$$

Clamped-Simply supported:

$$\begin{aligned}&W[0]=0,\ W[1]=0\\&\sum_{k=\rho}^{\infty}W[k]=0,\ \sum_{k=0}^{\infty}k[k-1]\ W[k]=0\end{aligned} \tag{30c}$$

By using Eq. (29) and with the transformed boundary conditions one arrives at the following eigenvalue problem

$$\begin{bmatrix}A_{11} & A_{12}\\ A_{21} & A_{22}\end{bmatrix}[C]=0 \tag{31}$$

where $[C]$ correspond to the missing boundary conditions at x=0. For the non-trivial solutions of Eq. (31), it is necessary that the determinant of the coefficient matrix is equal to zero

Table 3 Material properties of Al and Si (Miller *et al*. 2000)

Material	E (Gpa)	ρ (kg/m^3)	v	E_s (N/M)	τ_0 (N/M)	α_x (1/k)*10^{-6}
Al	70	2700	0.3	5.1882	0.9108	8.4
Si	210	2370	0.24	-10.6543	0.6048	2.56

Table 4 Comparison of the non-dimensional fundamental natural frequencies ($\hat{\omega} = \omega L^2 \sqrt{\rho A / EI}$) of simply supported beams

L/D	μ	Thai (2012)	Reddy (2007)	Present paper
10	0	9.8293	9.8696	9.86960440
	1	9.3774	9.4159	9.41588108
	2	8.9826	9.0195	9.01948110
	3	8.6338	8.6693	8.66926898
	4	8.3228	8.3569	8.35691990
20	0	9.8595	9.8696	9.86960440
	1	9.4062	9.4159	9.41588108
	2	9.0102	9.0195	9.01948110
	3	8.6604	8.6693	8.66926898
	4	8.3483	8.3569	8.35691990
100	0	9.8692	9.8696	9.86960440
	1	9.4155	9.4159	9.41588108
	2	9.0191	9.0195	9.01948110
	3	8.6689	8.6693	8.66926898
	4	8.3566	8.3569	8.35691990

$$\begin{vmatrix} A_{11} & A_{12} \\ A_{21} & A_{22} \end{vmatrix} = 0 \tag{32}$$

Solution of Eq. (32) is simply a polynomial root finding problem. Many techniques such as Newton's method, Laguerre's method, etc. can be used to find the roots of this frequency equation.

5. Numerical results and discussions

In this study, a nanotube with circular cross-section is assumed to obtain governing equations. The numerical results are obtained for Aluminum (Al) with crystallographic direction of [1 1 1] and Silicon (Si) with crystallographic direction of [1 0 0]. The material properties for Aluminum and silicon nanotube and the relevant properties is considered as shown in Table 3. First of all, to approve the validity of equations and solution method the nonlocal natural frequencies and critical buckling loads of nanotubes are compared will those in well-known studies. In Tables 4 and 5 the non-dimensional fundamental natural frequencies $\hat{\omega} = \omega L^2 \sqrt{\rho A / EI}$, and the non-dimensional critical buckling load, are listed and compared with results given by Reddy (2007) and Thai

Table 5 Comparison of the non-dimensional critical buckling loads ($\bar{N}_{cr}^{0} = N_m (L^2/EI)$) of simply supported beams

L/D	μ	Thai (2012)	Reddy (2007)	Present paper
10	0	9.8696	9.8696	9.86960440
	1	8.9830	8.9830	8.98301623
	2	8.2426	8.2426	8.24258361
	3	7.6149	7.6149	7.61491765
	4	7.0761	7.0761	7.07607999
20	0	9.8696	9.8696	9.86960440
	1	8.9830	8.9830	8.98301623
	2	8.2426	8.2426	8.24258361
	3	7.6149	7.6149	7.61491765
	4	7.0761	7.0761	7.07607999
100	0	9.8696	9.8696	9.86960440
	1	8.9830	8.9830	8.98301623
	2	8.2426	8.2426	8.24258361
	3	7.6149	7.6149	7.61491765
	4	7.0761	7.0761	7.07607999

Table 6 Critical buckling load corresponding first mode with various boundary condition with changing temperature (L/D=10, Ro=2Ri)

μ	θ	S-S			C-S			C-C		
		NE (both)	NSE (Al)	NSE (Si)	NE (both)	NSE (Al)	NSE (Si)	NE (both)	NSE (Al)	NSE (Si)
0	0	9.8696	42.9089	34.2707	20.1907	53.2300	44.5918	39.4784	72.5177	63.8795
	10	9.8698	42.9091	34.2708	20.1909	53.2302	44.5919	39.4786	72.5179	63.8796
	20	9.8700	42.9093	34.2708	20.1911	53.2304	44.5920	39.4788	72.5181	63.8796
	50	9.8706	42.9099	34.2710	20.1918	53.2311	44.5921	39.4795	72.5188	63.8798
	100	9.8717	42.9110	34.2712	20.1928	53.2321	44.5923	39.4805	72.5198	63.8800
1	0	8.98302	42.0223	33.3841	16.7989	49.8382	41.2000	28.3043	61.3436	52.7054
	10	8.98323	42.0225	33.3842	16.7991	49.8384	41.2001	28.3045	61.3438	52.7055
	20	8.98344	42.0227	33.3842	16.7993	49.8386	41.2002	28.3047	61.344	52.7055
	50	8.9840	42.0234	33.3844	16.8000	49.8392	41.2003	28.3054	61.3447	52.7057
	100	8.9851	42.0244	33.3846	16.8010	49.8403	41.2005	28.3064	61.3457	52.7059
2	0	8.2425	41.2819	32.6437	14.3828	47.4220	38.7839	22.0603	55.0996	46.4614
	10	8.2427	41.2821	32.6437	14.3830	47.4223	38.7840	22.0605	55.0998	46.4615
	20	8.2430	41.2823	32.6438	14.3832	47.4225	38.7841	22.0607	55.1000	46.4615
	50	8.2436	41.2829	32.6439	14.3838	47.4231	38.7842	22.0614	55.1006	46.4616
	100	8.2446	41.2840	32.6442	14.3849	47.4241	38.7844	22.0624	55.1017	46.4619
3	0	7.6149	40.6542	32.0160	12.5742	45.6135	36.9753	18.0733	51.1126	42.4744
	10	7.6151	40.6544	32.0161	12.5744	45.6137	36.9754	18.0735	51.1129	42.4744
	20	7.6153	40.6546	32.0161	12.5747	45.6139	36.9755	18.0737	51.1133	42.4745
	50	7.6159	40.6553	32.0163	12.5753	45.6146	36.9756	18.0743	51.1137	42.4746
	100	7.6170	40.6563	32.0165	12.5763	45.6156	36.9758	18.0754	51.1145	42.4749

*NE: Nonlocal effect, NSE: coupling nonlocal and surface effect

Table 7 Natural frequency corresponding first mode with various boundary conditions with changing temperature (L/D=10, Ro=2Ri)

μ	θ	S-S			C-S			C-C		
		NE (both)	NSE(Al)	NSE(Si)	NE (both)	NSE(Al)	NSE(Si)	NE (both)	NSE(Al)	NSE(Si)
0	0	9.8696	20.5790	18.3913	15.4182	24.6970	22.6692	22.3733	29.9999	28.2272
	10	9.8687	20.5789	18.3912	15.4169	24.6970	22.6691	22.3714	29.9999	28.2272
	20	9.8678	20.5789	18.3912	15.4156	24.6970	22.6691	22.3696	29.9999	28.2272
	50	9.8652	20.5788	18.3912	15.4117	24.6969	22.6691	22.3640	29.9998	28.2271
	100	9.8608	20.5786	18.3911	15.4051	24.6967	22.6690	22.3548	29.9996	28.2271
1	0	9.4158	20.3653	18.1518	14.5992	24.9139	22.6895	21.1090	30.8606	28.6439
	10	9.4150	20.3652	18.1518	14.598	24.9138	22.6895	21.1073	30.8606	28.6439
	20	9.4142	20.3652	18.1518	14.5967	24.9138	22.6895	21.1055	30.8605	28.6439
	50	9.4116	20.3651	18.1517	14.593	24.9137	22.6895	21.1003	30.8604	28.6439
	100	9.4075	20.3649	18.1517	14.5868	24.9135	22.6894	21.0916	30.8602	28.6438
2	0	9.0194	20.1850	17.9494	13.8962	25.0654	22.6911	20.0328	31.5082	28.9561
	10	9.0186	20.1850	17.9494	13.895	25.0654	22.6911	20.0311	31.5082	28.9561
	20	9.0178	20.1850	17.9494	13.8938	25.0653	22.6910	20.0295	31.5081	28.9561
	50	9.0154	20.1848	17.9493	13.8903	25.0652	22.6910	20.0245	31.508	28.9560
	100	9.0114	20.1846	17.9492	13.8844	25.0650	22.6909	20.0162	31.5078	28.9560
3	0	8.6692	20.0310	17.7760	13.2843	25.1767	22.6830	19.1029	32.014	29.1982
	10	8.6685	20.0310	17.7760	13.2832	25.1767	22.6830	19.1013	32.0139	29.1982
	20	8.6677	20.0309	17.7760	13.2821	25.1767	22.6829	19.0998	32.0139	29.1981
	50	8.6654	20.0308	17.7759	13.2787	25.1765	22.6829	19.0950	32.0137	29.1981
	100	8.6615	20.0306	17.7758	13.2731	25.1763	22.6828	19.0871	32.0135	29.1980

*NE: Nonlocal effect, NSE: coupling nonlocal and surface effect

(2012).

It is observed that resultant natural frequencies matched very well with those given in Reddy (2007), Thai (2012). It is also shown that by increasing the nonlocal parameter the natural frequency and buckling load decrease. The reason is that the presence of the nonlocal effect tends to decrease the stiffness of the nanostructures and hence decreases the values of natural frequencies and buckling loads.

Next, the critical buckling loads $\bar{N}_{cr}^{0}$ and natural frequencies $\hat{\omega}$ corresponding the first mode for a nanotube with various boundary conditions are presented in Tables 6-7 for constant value of aspect ratio L/D=10 and various nonlocal parameter μ by changing temperature. The nonlocal parameters $\mu=(e_0a)^2$ are taken as 0, 1, 2, 3, and 4 nm^2. It should be noted that $\mu=0$ corresponds to local beam theory. It should be noted that when the value nonlocal parameter is zero the results are obtained for the local beam theory. The results show that the surface effects increase the stiffness of nanotubes, and also by increasing the temperature the value of natural frequency decreases while the critical buckling increases.

The critical buckling load is calculated for different nanotube thickness for different temperatures which is presented in Tables 8-10. As it is shown in Tables 8-11 by increasing the

thickness of nanotube for different nonlocal parameters the value of critical buckling load decreases for all values of temperature which are presented (θ=0,50,100). And also it van be observed that for all values of nonlocal parameters and thicknesses the increase in temperature reduces the value of critical buckling load.

Table 8 Critical buckling load corresponding with various boundary conditions (L/D=10 θ=0)

R_o/R_i	μ=0 nm^2			μ=1 nm^2			μ=2 nm^2		
	NE(both)	NSE(Al)	NSE(Si)	NE(both)	NSE(Al)	NSE(Si)	NE(both)	NSE(Al)	NSE(Si)
					S-S				
2	9.8696	42.9089	34.2707	8.9830	42.0223	33.3841	8.2425	41.2819	32.6437
5	9.8696	43.0843	29.7825	8.9830	42.1977	28.8959	8.2425	41.4573	28.1555
10	9.8696	43.1395	29.6369	8.9830	42.2530	28.7503	8.2425	41.5125	28.0099
15	9.8696	43.1466	29.6247	8.9830	42.2600	28.7381	8.2425	41.5196	27.9977
20	9.8696	43.1484	29.622	8.9830	42.2618	28.7354	8.2425	41.5214	27.9949
50	9.8696	43.1497	29.6202	8.9830	42.2632	28.7336	8.2425	41.5227	27.9931
100	9.8696	43.1498	29.6201	8.9830	42.2632	28.7335	8.2425	41.5228	27.9930
					C-S				
2	20.1907	53.2300	44.5918	16.7989	49.8382	41.2000	14.3828	47.4220	38.7839
5	20.1907	53.4054	40.1036	16.7989	50.0136	36.7118	14.3828	47.5975	34.2957
10	20.1907	53.4607	39.9580	16.7989	50.0689	36.5662	14.3828	47.6527	34.1500
15	20.1907	53.4677	39.9458	16.7989	50.0759	36.5540	14.3828	47.6597	34.1379
20	20.1907	53.4695	39.9431	16.7989	50.0777	36.5513	14.3828	47.6616	34.1351
50	20.1907	53.4709	39.9413	16.7989	50.0791	36.5495	14.3828	47.6629	34.1333
100	20.1907	53.4710	39.9412	16.7989	50.0791	36.5494	14.3828	47.6630	34.1332
					C-C				
2	39.4784	72.5177	63.8795	28.3043	61.3436	52.7054	22.0603	55.0996	46.4614
5	39.4784	72.6931	59.3913	28.3043	61.5190	48.2172	22.0603	55.2750	41.9732
10	39.4784	72.7484	59.2457	28.3043	61.5743	48.0716	22.0603	55.3302	41.8276
15	39.4784	72.7554	59.2335	28.3043	61.5813	48.0594	22.0603	55.3373	41.8154
20	39.4784	72.7572	59.2308	28.3043	61.5831	48.0567	22.0603	55.3391	41.8126
50	39.4784	72.7586	59.2290	28.3043	61.5845	48.0549	22.0603	55.3404	41.8109
100	39.4784	72.7586	59.2289	28.3043	61.5845	48.0548	22.0603	55.3405	41.8108

Table 9 Critical buckling load corresponding with various boundary conditions (L/D=10, θ=50)

R_o/R_i	μ=0 nm^2			μ=1 nm^2			μ=2 nm^2		
	NE(both)	NSE(Al)	NSE(Si)	NE(both)	NSE(Al)	NSE(Si)	NE(both)	NSE(Al)	NSE(Si)
					S-S				
2	9.87065	42.9099	34.271	8.98407	42.0234	33.3844	8.24363	41.2829	32.6439
5	9.87065	43.0853	29.7828	8.98407	42.1988	28.8962	8.24363	41.4583	28.1557
10	9.87065	43.1406	29.6371	8.98407	42.254	28.7505	8.24363	41.5136	28.0101
15	9.87065	43.1476	29.625	8.98407	42.261	28.7384	8.24363	41.5206	27.9979
20	9.87065	43.1495	29.6222	8.98407	42.2629	28.7356	8.24363	41.5225	27.9952
50	9.87065	43.1508	29.6204	8.98407	42.2642	28.7338	8.24363	41.5238	27.9934
100	9.87065	43.1509	29.6203	8.98407	42.2643	28.7337	8.24363	41.5239	27.9933

Table 9 Continued

C-S									
2	20.1918	53.2311	44.5921	16.8	49.8392	41.2003	14.3838	47.4231	38.7841
5	20.1918	53.4065	40.1039	16.8	50.0147	36.7121	14.3838	47.5985	34.2959
10	20.1918	53.4617	39.9583	16.8	50.0699	36.5664	14.3838	47.6538	34.1503
15	20.1918	53.4688	39.9461	16.8	50.0769	36.5543	14.3838	47.6608	34.1381
20	20.1918	53.4706	39.9433	16.8	50.0788	36.5515	14.3838	47.6626	34.1354
50	20.1918	53.4719	39.9415	16.8	50.0801	36.5497	14.3838	47.664	34.1336
100	20.1918	53.472	39.9414	16.8	50.0802	36.5496	14.3838	47.664	34.1335
C-C									
2	39.4795	72.5188	63.8798	28.3054	61.3447	52.7057	22.0614	55.1006	46.4616
5	39.4795	72.6942	59.3916	28.3054	61.5201	48.2175	22.0614	55.276	41.9735
10	39.4795	72.7494	59.2459	28.3054	61.5753	48.0718	22.0614	55.3313	41.8278
15	39.4795	72.7564	59.2338	28.3054	61.5824	48.0597	22.0614	55.3383	41.8157
20	39.4795	72.7583	59.231	28.3054	61.5842	48.0569	22.0614	55.3402	41.8129
50	39.4795	72.7596	59.2292	28.3054	61.5855	48.0551	22.0614	55.3415	41.8111
100	39.4795	72.7597	59.2291	28.3054	61.5856	48.055	22.0614	55.3416	41.811

Table 10 Critical buckling load corresponding with various boundary conditions (L/D=10, θ=100)

R_o/R_i	μ=0 nm^2			μ=1 nm^2			μ=2 nm^2		
	NE(both)	NSE(Al)	NSE(Si)	NE(both)	NSE(Al)	NSE(Si)	NE(both)	NSE(Al)	NSE(Si)
S-S									
2	9.8717	42.9110	34.2712	8.9851	42.0244	33.3846	8.2446	41.2840	32.6442
5	9.8717	43.0864	29.7830	8.9851	42.1998	28.8964	8.2446	41.4594	28.1560
10	9.8717	43.1416	29.6374	8.9851	42.2551	28.7508	8.2446	41.5146	28.0104
15	9.8717	43.1487	29.6252	8.9851	42.2621	28.7386	8.2446	41.5217	27.9982
20	9.8717	43.1505	29.6224	8.9851	42.2639	28.7359	8.2446	41.5235	27.9954
50	9.8717	43.1518	29.6207	8.9851	42.2653	28.7341	8.2446	41.5248	27.9936
100	9.8717	43.1519	29.6206	8.9851	42.2653	28.7340	8.2446	41.5249	27.9935
C-S									
2	20.1928	53.2321	44.5923	16.8010	49.8403	41.2005	14.3849	47.4241	38.7844
5	20.1928	53.4075	40.1041	16.8010	50.0157	36.7123	14.3849	47.5996	34.2962
10	20.1928	53.4628	39.9585	16.8010	50.0710	36.5667	14.3849	47.6548	34.1505
15	20.1928	53.4698	39.9463	16.8010	50.0780	36.5545	14.3849	47.6618	34.1384
20	20.1928	53.4716	39.9436	16.8010	50.0798	36.5517	14.3849	47.6637	34.1356
50	20.1928	53.4730	39.9418	16.8010	50.0812	36.5500	14.3849	47.6650	34.1338
100	20.1928	53.4731	39.9417	16.8010	50.0812	36.5499	14.3849	47.6651	34.1337
C-C									
2	39.4805	72.5198	63.8800	28.3064	61.3457	52.7059	22.0624	55.1017	46.4619
5	39.4805	72.6952	59.3918	28.3064	61.5211	48.2177	22.0624	55.2771	41.9737
10	39.4805	72.7505	59.2462	28.3064	61.5764	48.0721	22.0624	55.3323	41.8281
15	39.4805	72.7575	59.2340	28.3064	61.5834	48.0599	22.0624	55.3394	41.8159
20	39.4805	72.7593	59.2313	28.3064	61.5852	48.0572	22.0624	55.3412	41.8131
50	39.4805	72.7607	59.2295	28.3064	61.5866	48.0554	22.0624	55.3425	41.8114
100	39.4805	72.7607	59.2294	28.3064	61.5866	48.0553	22.0624	55.3426	41.8113

And also the influence of nanotube thickness is investigated on the fundamental natural frequencies in Tables 11-13. It can be seen that for different values of nonlocal parameter and temperature the increase in thickness cause decrease in value of natural frequency for Si nanotube while the value of natural frequency in Al increases for all boundary conditions.

Table 11 Natural frequency corresponding with various boundary condition (L/D=10, θ=0)

R_o/R_i	μ=0 nm^2			μ=1 nm^2			μ=2 nm^2		
	NE (both)	NSE (Al)	NSE (Si)	NE (both)	NSE (Al)	NSE (Si)	NE (both)	NSE (Al)	NSE (Si)
S-S									
2	9.8696	20.5790	18.3913	9.4158	20.3653	18.1518	9.0194	20.1850	17.9494
5	9.8696	20.6210	17.1447	9.4158	20.4077	16.8876	9.0194	20.2279	16.6698
10	9.8696	20.6342	17.1028	9.4158	20.4211	16.8450	9.0194	20.2413	16.6267
15	9.8696	20.6359	17.0992	9.4158	20.4228	16.8414	9.0194	20.2431	16.6231
20	9.8696	20.6363	17.0984	9.4158	20.4232	16.8406	9.0194	20.2435	16.6222
50	9.8696	20.6366	17.0979	9.4158	20.4235	16.8401	9.0194	20.2438	16.6217
100	9.8696	20.6367	17.0979	9.4158	20.4236	16.8401	9.0194	20.2439	16.6217
C-S									
2	15.4182	22.6692	24.6970	14.5992	22.6895	24.9139	13.8962	22.6911	25.0654
5	15.4182	21.5334	24.7363	14.5992	21.4397	24.9569	13.8962	21.3518	25.1113
10	15.4182	21.4954	24.7487	14.5992	21.3979	24.9705	13.8962	21.3070	25.1257
15	15.4182	21.4923	24.7503	14.5992	21.3944	24.9722	13.8962	21.3032	25.1275
20	15.4182	21.4915	24.7507	14.5992	21.3936	24.9726	13.8962	21.3023	25.1280
50	15.4182	21.4911	24.7510	14.5992	21.3931	24.9730	13.8962	21.3018	25.1284
100	15.4182	21.4911	24.7510	14.5992	21.3931	24.9730	13.8962	21.3018	25.1284
C-C									
2	22.3733	29.9999	28.2272	21.1090	30.8606	28.6439	20.0328	31.5082	28.9561
5	22.3733	30.0347	27.2550	21.1090	30.9039	27.4192	20.0328	31.5579	27.5358
10	22.3733	30.0457	27.2228	21.1090	30.9176	27.3785	20.0328	31.5735	27.4884
15	22.3733	30.0471	27.2201	21.1090	30.9193	27.3751	20.0328	31.5755	27.4845
20	22.3733	30.0474	27.2195	21.1090	30.9198	27.3743	20.0328	31.5760	27.4836
50	22.3733	30.0477	27.2191	21.1090	30.9201	27.3738	20.0328	31.5764	27.4830
100	22.3733	30.0477	27.2191	21.1090	30.9201	27.3738	20.0328	31.5764	27.4830

Table 12 Natural frequency corresponding with various boundary condition (L/D=10, θ=50)

R_o/R_i	μ=0 nm^2			μ=1 nm^2			μ=2 nm^2		
	NE (both)	NSE (Al)	NSE (Si)	NE (both)	NSE (Al)	NSE (Si)	NE (both)	NSE (Al)	NSE (Si)
S-S									
2	9.86521	20.5788	18.3912	9.41169	20.3651	18.1517	9.01547	20.1848	17.9493
5	9.86521	20.6208	17.1447	9.41169	20.4075	16.8875	9.01547	20.2277	16.6698
10	9.86521	20.634	17.1027	9.41169	20.4209	16.8449	9.01547	20.2412	16.6266
15	9.86521	20.6357	17.0992	9.41169	20.4226	16.8414	9.01547	20.2429	16.623
20	9.86521	20.6361	17.0984	9.41169	20.423	16.8406	9.01547	20.2433	16.6222
50	9.86521	20.6364	17.0979	9.41169	20.4233	16.84	9.01547	20.2436	16.6216
100	9.86521	20.6365	17.0978	9.41169	20.4234	16.84	9.01547	20.2437	16.6216

Table 12 Continued

C-S									
2	15.4162	22.6691	24.6969	14.5973	22.6895	24.9137	13.8944	22.691	25.0652
5	15.4162	21.5333	24.7362	14.5973	21.4397	24.9567	13.8944	21.3518	25.1111
10	15.4162	21.4954	24.7485	14.5973	21.3979	24.9703	13.8944	21.3069	25.1255
15	15.4162	21.4922	24.7501	14.5973	21.3944	24.972	13.8944	21.3031	25.1273
20	15.4162	21.4915	24.7505	14.5973	21.3936	24.9724	13.8944	21.3023	25.1278
50	15.4162	21.491	24.7508	14.5973	21.3931	24.9728	13.8944	21.3017	25.1281
100	15.4162	21.491	24.7508	14.5973	21.393	24.9728	13.8944	21.3017	25.1282
C-C									
2	22.364	29.9998	28.2271	21.1003	30.8604	28.6439	20.0245	31.508	28.956
5	22.364	30.0346	27.2549	21.1003	30.9037	27.4191	20.0245	31.5577	27.5357
10	22.364	30.0455	27.2227	21.1003	30.9174	27.3784	20.0245	31.5733	27.4883
15	22.364	30.0469	27.2201	21.1003	30.9191	27.375	20.0245	31.5753	27.4844
20	22.364	30.0473	27.2194	21.1003	30.9196	27.3743	20.0245	31.5758	27.4835
50	22.364	30.0475	27.219	21.1003	30.9199	27.3738	20.0245	31.5762	27.4829
100	22.364	30.0476	27.219	21.1003	30.9199	27.3737	20.0245	31.5762	27.4829

Table 13 Natural frequency corresponding with various boundary condition (L/D=10, θ=100)

R_o/R_i	μ=0 nm^2			μ=1 nm^2			μ=2 nm^2		
	NE (both)	NSE (Al)	NSE (Si)	NE (both)	NSE (Al)	NSE (Si)	NE (both)	NSE (Al)	NSE (Si)
S-S									
2	9.8608	20.5786	18.3911	9.4075	20.3649	18.1517	9.0114	20.1846	17.9492
5	9.8608	20.6206	17.1446	9.4075	20.4073	16.8875	9.0114	20.2275	16.6697
10	9.8608	20.6338	17.1026	9.4075	20.4207	16.8449	9.0114	20.2410	16.6265
15	9.8608	20.6355	17.0991	9.4075	20.4224	16.8413	9.0114	20.2427	16.6229
20	9.8608	20.6359	17.0983	9.4075	20.4228	16.8405	9.0114	20.2431	16.6221
50	9.8608	20.6363	17.0978	9.4075	20.4231	16.8400	9.0114	20.2434	16.6216
100	9.8608	20.6363	17.0978	9.4075	20.4232	16.8399	9.0114	20.2435	16.6215
C-S									
2	15.4142	22.6690	24.6967	14.5954	22.6894	24.9135	13.8926	22.6909	25.065
5	15.4142	21.5333	24.7360	14.5954	21.4396	24.9565	13.8926	21.3517	25.1108
10	15.4142	21.4953	24.7484	14.5954	21.3978	24.9701	13.8926	21.3068	25.1253
15	15.4142	21.4921	24.7499	14.5954	21.3943	24.9718	13.8926	21.3030	25.1271
20	15.4142	21.4914	24.7503	14.5954	21.3935	24.9722	13.8926	21.3022	25.1276
50	15.4142	21.4910	24.7506	14.5954	21.3930	24.9726	13.8926	21.3016	25.1279
100	15.4142	21.4909	24.7507	14.5954	21.3930	24.9726	13.8926	21.3016	25.1280
C-C									
2	22.3548	29.9996	28.2271	21.0916	30.8602	28.6438	20.0162	31.5078	28.9560
5	22.3548	30.0344	27.2549	21.0916	30.9035	27.4191	20.0162	31.5574	27.5356
10	22.3548	30.0454	27.2227	21.0916	30.9172	27.3784	20.0162	31.5731	27.4883
15	22.3548	30.0467	27.2200	21.0916	30.9189	27.3750	20.0162	31.5751	27.4843
20	22.3548	30.0471	27.2194	21.0916	30.9194	27.3742	20.0162	31.5756	27.4834
50	22.3548	30.0474	27.2190	21.0916	30.9197	27.3737	20.0162	31.5759	27.4828
100	22.3548	30.0474	27.2190	21.0916	30.9197	27.3737	20.0162	31.5760	27.4828

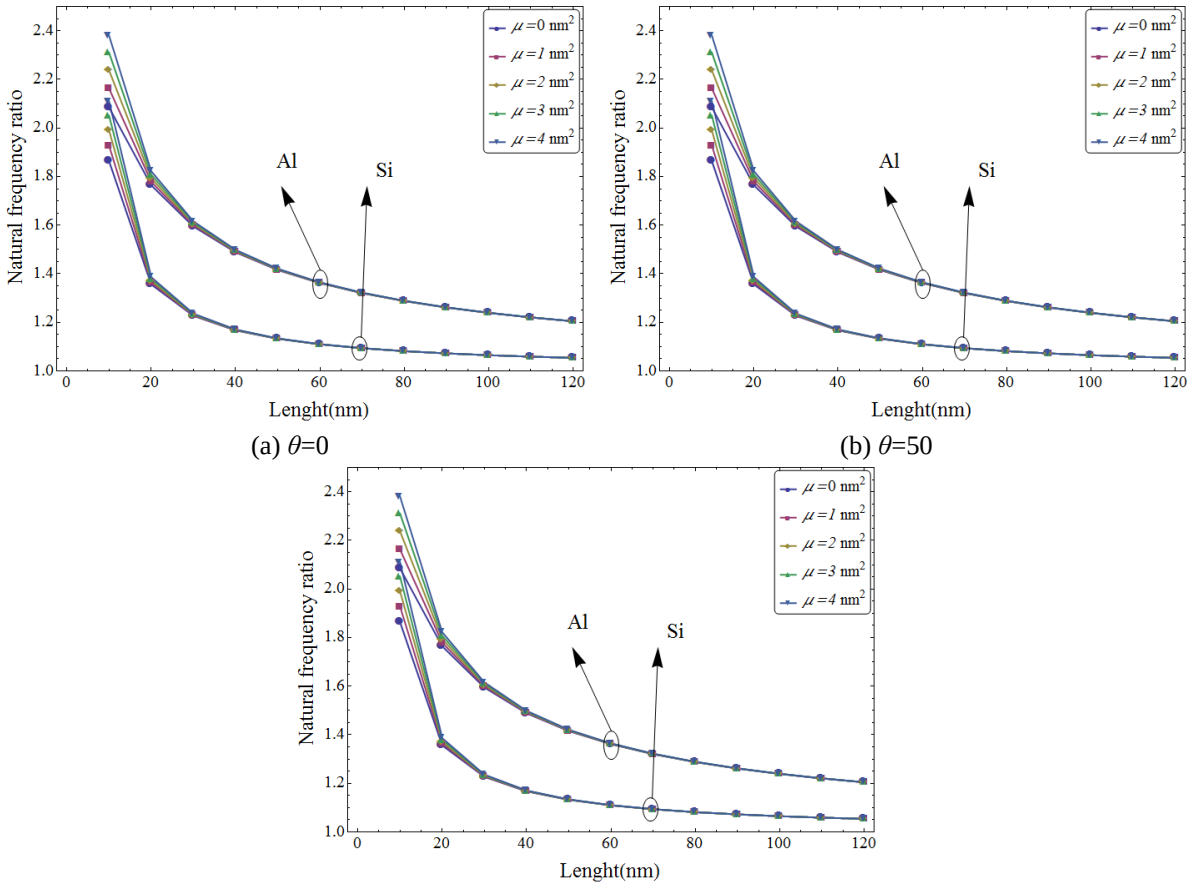

(a) θ=0 (b) θ=50

(c) θ=100

Fig. 2 Variation of natural frequency ratio versus length for Al and Si materials

It can be observed that by increasing the nonlocal parameters for a constant value of thickness the natural frequency decreases for both Al and Si. And also by comparing the natural frequencies in a constant situation, it can be seen that increasing the temperate decreases the value of natural frequency. In the following the influence of surface effect will be studied, and the non-dimensional free vibration frequency and critical buckling load ratio of nanotubes made of Al and Si, normalized with respect to the fundamental natural frequency and critical buckling load by ignoring the surface effects. In Figs. 2 and 3 the variations of the natural frequencies and critical buckling loads ratio with respect to the Length of nanotube are plotted for various boundary condition and different nonlocal parameters for different values of temperature, respectively. It is shown from Figs. 2 and 3 that in constant length of nanotube with the increase in nonlocal parameter, the natural frequencies and critical buckling loads ratio increase. On the other hand, when the nonlocal parameter is increased, the surface effects play a significant role in the vibration and buckling behavior of nanotube

In Fig. 4 and Fig. 5 the variation of the natural frequencies and critical buckling loads ratio wuth respect to the aspect ratio are investigated for Al and Si nanotube. All the results are calculated for simply supported nanotube for various temperature values (θ=0,50,100). It is

observed that in constant length of nanotube with the increase in the aspect ratio, the natural frequencies and critical buckling loads ratio increase. On the other hand, when the aspect ratio is increased, the surface effects play a significant role in the vibration and buckling behavior of

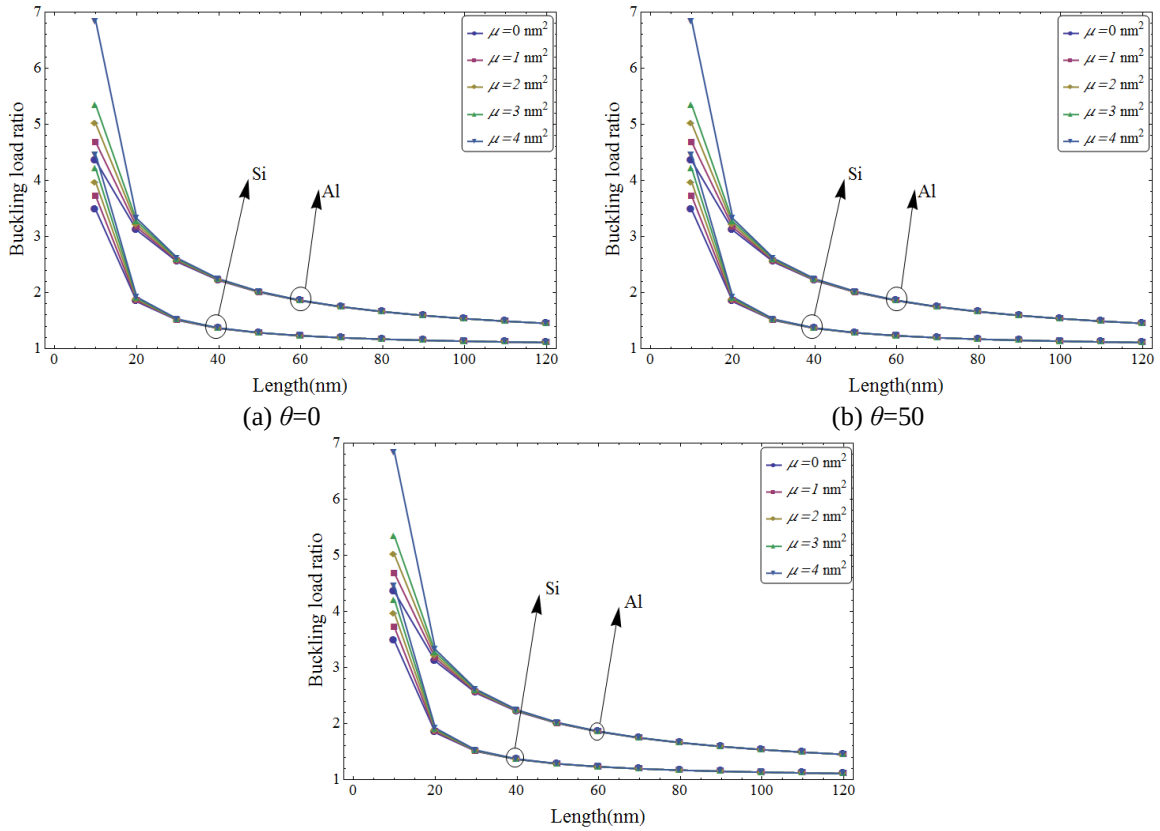

(a) θ=0 (b) θ=50

(c) θ=100

Fig. 3 Variation of critical buckling ratio versus length for Al and Si materials for S-S

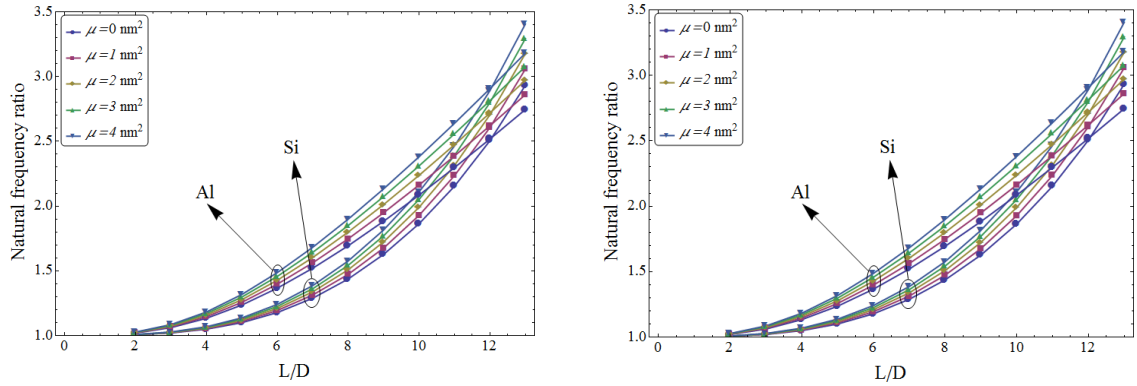

(a) θ=0 (b) θ=50

Fig. 4 Variation of natural frequency ratio versus aspect ratio(L/D) for Al and Si materials for S-S

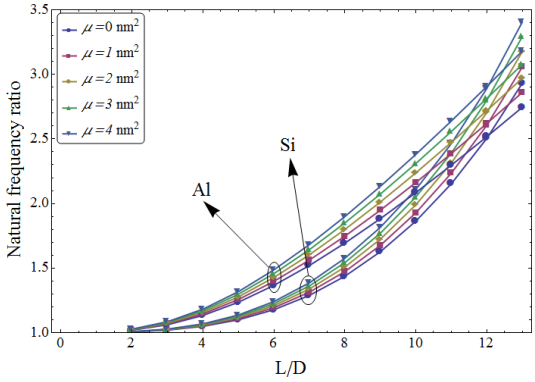

(c) θ=100

Fig. 4 Continued

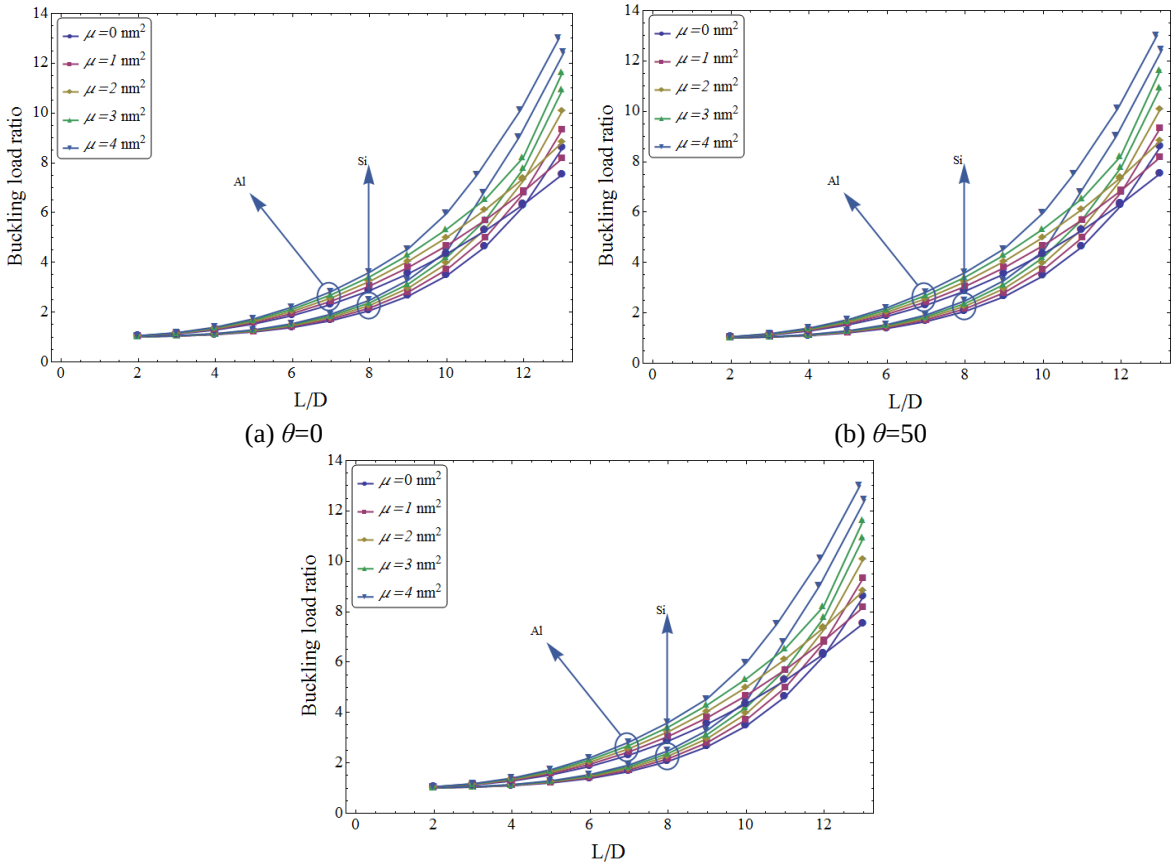

(a) θ=0 (b) θ=50

(c) θ=100

Fig. 5 Critical buckling load ratio versus aspect ratio(L/D) for Al and Si materials for S-S

nanotube. In addition, this figures illustrate that increasing the nonlocal parameter cause increase of natural frequency and critical buckling load ratio.

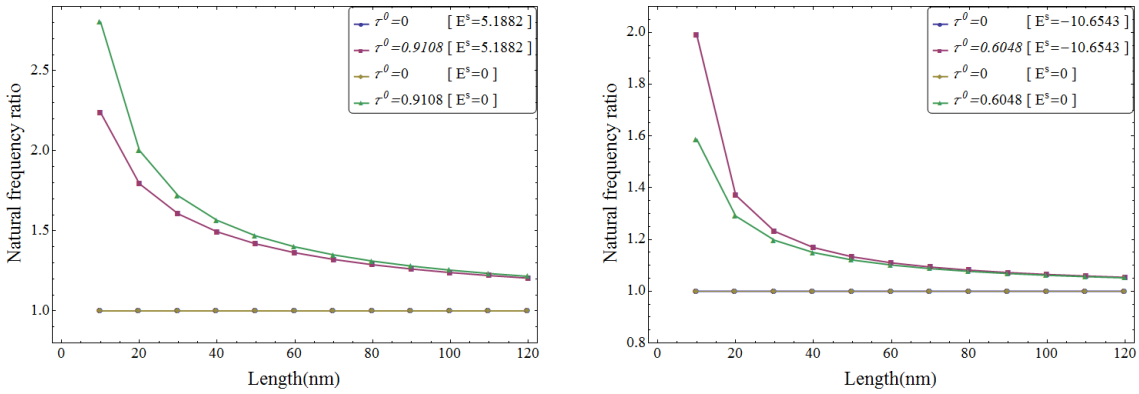

(a) Material of Al (b) Material of Si

Fig. 6 Variation of natural frequency ratio of simply supported nanotube versus length corresponding to magnitudes of different τ^o and E^s

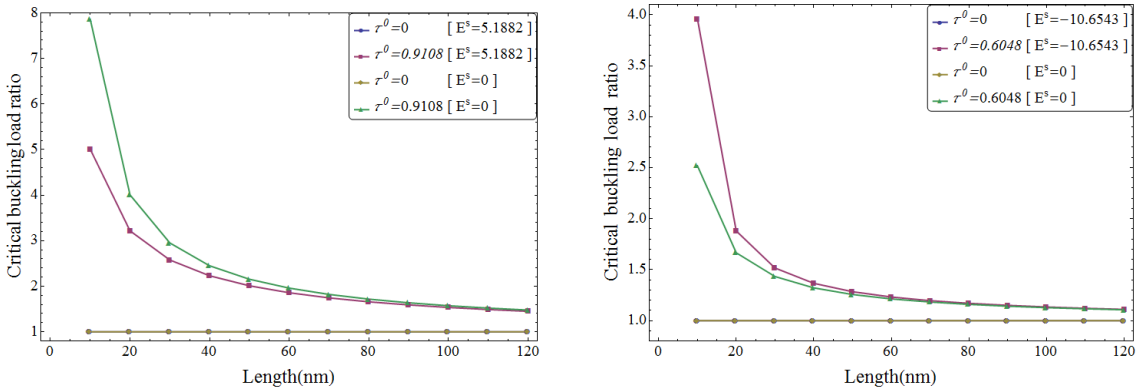

(a) Material of Al (b) Material of Si

Fig. 7 Variation of critical buckling load of simply supported nanotube versus length corresponding to magnitudes of different τ^o and E^s

Finally, the influence of surface effects separately and simultaneously are shown in Figs. 6 and 7. All the results are calculated for simply supported nanotube for different cases of surface stress and surface elasticity when L/D=10 and μ=2 nm^2. It is observed from these figures, that in the case that the surface stress is ignored the surface elasticity has no effect on the natural frequencies. But since surface stress is nonzero, value of surface elasticity play an important in nanostructures. Positive surface elasticity softens nanotube while negative surface elasticity stiffens nanotube. But surface stress lonely is important and effective even without consideration of surface elasticity and natural frequencies and critical buckling loads ratio is increased.

6. Conclusions

In the present study the free vibration and critical buckling load nanotubes by considering surface and thermal effects in presence of nonlocal effect were studied. The motion equations

where obtained by Hamilton method in the framework of Euler-Bernoulli beam theory for various boundary conditions. The numerical results were obtained for both Aluminum with positive surface elasticity and Silicon with negative surface elasticity by utilizing DTM as a semi-analytical-numerical method. The results illustrated that:

- By increasing the size of nanotube the influence of surface effects decrease for all the values of nonlocal parameter.
- In the case that the aspect ratio increase the influence of surface effects increase, too
- When the effect of thermal takes into account the value of natural frequencies decrease by increasing the temperature for Al and Si nanotubes, while the buckling load increase by increasing the temperature
- By the time the nonlocal parameter increase the value of natural frequencies and also the buckling loads by considering a constant value for the size variables, increase. The reason is that the nonlocal effect makes the nanobeam soften and the values of natural frequencies and buckling loads decrease.
- In should be found that the positive surface elasticity soften the nanotube while the negative surface elasticity makes the nanotube stiffer in presence of surface stress
- The results of the present model are validated by the literature and demonstrated that the present model can capture correctly the surface and nonlocal effects in presence of thermal effect in vibration and buckling analysis of nanotubes.

References

Abazari, R. and Abazari, R. (2010), "Numerical study of some coupled PDEs by using differential transformation method", *Proc. World Acad. Sci. Eng. Tech.*, **66**, 52-59.

Abbasi, S., Farhatnia, F. and Jazi, S.R. (2014), "A semi-analytical solution on static analysis of circular plate exposed to non-uniform axisymmetric transverse loading resting on Winkler elastic foundation", *Arch. Civil Mech. Eng.*, **14**(3), 476-488.

Amirian, B., Hosseini-Ara, R. and Moosavi, H. (2014), "Surface and thermal effects on vibration of embedded alumina nanobeams based on novel Timoshenko beam model", *Appl. Math. Mech.*, **35**(7), 875-886.

Ansari, R. and Sahmani, S. (2012), "Small scale effect on vibrational response of single-walled carbon nanotubes with different boundary conditions based on nonlocal beam models", *Commun. Nonlin. Sci. Numer. Simul.*, **17**(4), 1965-1979.

Eltaher, M.A., Mahmoud, F.F., Assie, A.E. and Meletis, E.I. (2013), "Coupling effects of nonlocal and surface energy on vibration analysis of nanobeams", *Appl. Math. Comput.*, **224**, 760-774.

Ebrahimi, F., Shaghaghi, G.R. and Boreiry, M. (2015a), "A semi-analytical evaluation of surface and nonlocal effects on buckling and vibrational characteristics of nanotubes with various boundary conditions", *Int. J. Struct. Stab. Dyn.*, 1550023.

Ebrahimi, F. and Salari, E. (2015b), "Effect of various thermal loadings on buckling and vibrational characteristics of nonlocal temperature-dependent FG nanobeams", *Mech. Adv. Mater. Struct.*, 1-58. (Accepted)

Eringen, A.C. and Edelen, D.G.B. (1972), "On nonlocal elasticity", *Int. J. Eng. Sci.*, **10**(3), 233-248.

Guo, J.G. and Zhao, Y.P. (2007), "The size-dependent bending elastic properties of nanobeams with surface effects", *Nanotechnol.*, **18**(29), 295701.

Gheshlaghi, B. and Hasheminejad, S.M. (2011), "Surface effects on nonlinear free vibration of nanobeams", *Compos. Part B: Eng.*, **42**(4), 934-937.

He, L.H., Lim, C.W. and Wu, B.S. (2004), "A continuum model for size-dependent deformation of elastic

films of nano-scale thickness", *Int. J. Solid. Struct.*, **41**(3), 847-857.
Hosseini-Hashemi, S., Fakher, M. and Nazemnezhad, R. (2013a), "Surface effects on free vibration analysis of nanobeams using nonlocal elasticity: a comparison between Euler-Bernoulli and Timoshenko", *J. Solid. Mech.*, **5**(3), 290-304.
Hosseini-Hashemi, S. and Nazemnezhad, R. (2013b), "An analytical study on the nonlinear free vibration of functionally graded nanobeams incorporating surface effects", *Compos. Part B: Eng.*, **52**, 199-206.
Zhou, J.K. (1986), *Differential Transformation and its Applications for Electrical Circuits*, Huazhong University Press, Wuhan.
Malekzadeh, P. and Shojaee, M. (2013), "Surface and nonlocal effects on the nonlinear free vibration of non-uniform nanobeams", *Compos. Part B: Eng.*, **52**, 84-92.
Miller, R.E. and Shenoy, V.B. (2000), "Size-dependent elastic properties of nanosized structural elements", *Nanotechnol.*, **11**(3), 139.
Reddy, J.N. (2007), "Nonlocal theories for bending, buckling and vibration of beams", *Int. J. Eng. Sci.*, **45**(2), 288-307.
Shariyat, M. (2009), "Dynamic buckling of imperfect laminated plates with piezoelectric sensors and actuators subjected to thermo-electro-mechanical loadings, considering the temperature-dependency of the material properties", *Compos. Struct.*, **88**(2), 228-239.
Thai, H.T. (2012), "A nonlocal beam theory for bending, buckling, and vibration of nanobeams", *Int. J. Eng. Sci.*, **52**, 56-64.
Wang, Q. and Varadan, V.K. (2006), "Vibration of carbon nanotubes studied using nonlocal continuum mechanics", *Smart Mater. Struct.*, **15**(2), 659.
Wang, C.M., Zhang, Y.Y. and He, X.Q. (2007), "Vibration of nonlocal Timoshenko beams", *Nanotechnology*, **18**(10), 105401.
Wang, L., Ni, Q., Li, M. and Qian, Q. (2008), "The thermal effect on vibration and instability of carbon nanotubes conveying fluid", *Physica E: Low-dimen. Syst. Nanostruct.*, **40**(10), 3179-3182.
Wang, G.F. and Feng, X.Q. (2009), "Surface effects on buckling of nanowires under uniaxial compression", *Appl. Phys. Lett.*, **94**(14), 141913.
Zhang, Y.Q., Liu, X. and Liu, G.R. (2007), "Thermal effect on transverse vibrations of double-walled carbon nanotubes", *Nanotechnol.*, **18**(44), 445701.
Zhang, Y.Q., Liu, X. and Zhao, J.H. (2008), "Influence of temperature change on column buckling of multiwalled carbon nanotubes", *Phys. Lett. A*, **372**(10), 1676-1681.

CC